

# Cylindrical Gravitational Waves in Expanding Universes: Explicit Pulse Solutions

Robert H. Gowdy\*

*Department of Physics, Virginia Commonwealth University, Richmond, VA 23284-2000*

(Dated: October 3, 2007)

Solutions analogous to the Weber-Wheeler cylindrical pulse waves are found for the case of cylindrical gravitational waves in an expanding universe. These pulse solutions mimic the asymptotic properties of waves from an isolated source in three dimensions and can be used to test the far-field behavior of numerical simulation techniques.

## I. INTRODUCTION

Exact solutions representing cylindrical gravitational waves in an expanding (Kasner) empty universe were introduced in an earlier paper.[1] They are potentially useful as models for waves from compact sources in asymptotically flat spacetimes. One possible application of these exact solutions is to check how well numerical simulations handle the transition from the near-field zone to the far-field zone where gravitational radiation power can be identified.[2, 3, 4, 5]

A shortcoming of the solutions presented earlier is that they are in the form of integrals over wave amplitudes. Here, we will show that the Bonnor amplitude distribution[6] that leads to the Weber-Wheeler pulse[7] in the Einstein-Rosen cylindrical wave case is integrable in the expanding-universe case as well. The resulting expression for a cylindrical pulse in an expanding universe is slightly more complex than the Weber-Wheeler pulse because it involves an elliptic function of the first kind, but can still be evaluated with little effort.

The explicit pulse solutions do provide one surprise: The basis functions that make up these solutions have the desired asymptotic behavior near future null infinity, but the first solutions found by summing these basis functions do not. The resulting pulses are not well localized and fill the event horizon of the expanding universe. As a result, they are amplified by the expansion and fall off as  $\ln r/r$  instead of at the expected  $1/r$  rate. Fortunately, combinations of these Bonnor-type pulse solutions can produce localized pulse solutions that are not amplified and have the  $1/r$  behavior that is needed to mimic waves from a compact source.

Section II of this paper provides a brief summary of the key results of the earlier paper and expands on a brief remark in the earlier paper to display the Minkowski space background geometry for these solutions. Section III constructs the basic Bonnor pulse solution and discusses its properties. The localized pulses that could be used to test numerical algorithms are constructed and analyzed in Section IV. These localized pulses include some with two peaks, separated by a narrow notch that could be used to test a numerical simulation's ability to produce accurate waveforms in the far-field region.

## II. REVIEW

### A. The metric

The general family of exact solutions discussed in the previous paper[1] have the spacetime metrics

$$ds^2 = -e^{2a} dt^2 + e^{2a} dr^2 + e^{-2W} r^2 d\varphi^2 + e^{2W} t^2 dz^2 \quad (1)$$

where the cylindrical wave function,  $W$  is given as an integral over wave amplitudes and Bessel functions.

$$W(r, t) = \int_0^\infty dk [A(k) J_0(kt) + C(k) N_0(kt)] J_0(kr) \quad (2)$$

The amplitude  $A(k)$  corresponds to waves that are regular near the initial singularity of the spacetime while the amplitude  $C(k)$  corresponds to waves that are singular there. So long as the singular wave amplitudes  $C(k)$  satisfy one of the two possible regularity constraints

$$\int_0^\infty dk \frac{C(k)}{k} = 0; \pi, \quad (3)$$

---

\*Electronic address: rgowdy@vcu.edu

the remaining metric function  $a$  can be expressed as

$$a(x, t) = -W(x, t) + \int_0^x \frac{t^2 Z}{t^2 - r^2} r dr, \quad (4)$$

where

$$Z = (W_r^2 + W_t^2) - 2\frac{r}{t}W_r W_t - 2\frac{r}{t^2}W_r + \frac{2}{t}W_t. \quad (5)$$

In contrast to the Einstein-Rosen cylindrical wave solutions[7], an integral constraint

$$\int_0^\infty \frac{t^2 Z}{t^2 - r^2} r dr = 0. \quad (6)$$

may be imposed to ensure that these hypersurfaces are asymptotically flat (rather than conical) at spatial infinity.[1]

It is useful, for the purpose of scaling solutions, to assign both  $t$  and  $r$  the dimension of length. With that assignment, the functions  $W$  and  $a$  are dimensionless,  $k$  is an inverse length and the amplitude functions  $A(k)$  and  $C(k)$  scale as lengths.

### B. The background spacetime

The trivial solution  $a = W = 0$  corresponds to the spacetime metric

$$ds^2 = -dt^2 + dr^2 + r^2 d\varphi^2 + t^2 dz^2,$$

which may be regarded as describing a background geometry for these solutions. In terms of the new coordinates,  $X, Y, Z, T$  defined by

$$\begin{aligned} T &= t \cosh z, & Z &= t \sinh z \\ X &= r \cos \varphi, & Y &= r \sin \varphi \end{aligned}$$

this background metric is just

$$ds^2 = -dT^2 + dX^2 + dY^2 + dZ^2$$

and corresponds to a sector of flat Minkowski spacetime, as shown in fig. 1.

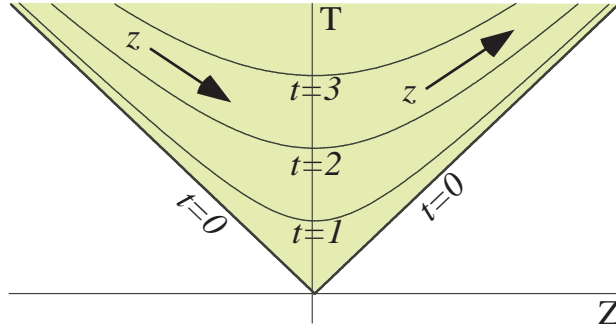


FIG.1 The effective background geometry for these solutions is the shaded region of flat Minkowski spacetime.

In this background geometry, the apparent singularity at  $t = 0$  is just a result of using space coordinates that are expanding in the  $Z$  direction. Thus it will sometimes be possible to extend these spacetimes past  $t = 0$  and identify translations in  $z$  with boosts in Minkowski space. This type of extension is similar to the Taub-NUT extension and is just the same as the familiar extension of Misner Space that provides a toy model of the Taub-NUT extension.[8, 9, 10] When such an extension is possible, the solution will correspond to one of the boost-rotation symmetric solutions considered by Bičák and Schmidt.[11] Even when an extension past  $t = 0$  is not possible, these solutions inherit the future asymptotic structure of Minkowski space, which is one way to understand how they can be asymptotically flat at future null infinity.[1]

### III. BONNOR PULSES

#### A. Integrating the Bonnor amplitude

The amplitudes  $A(k)$  and  $C(k)$  are arbitrary, subject only to the regularity constraint, Eq. 3. The pulse solutions that we wish to construct correspond to the choices

$$A(k) = \alpha e^{-\alpha k}$$

$$C(k) = 0.$$

where  $\alpha$  is the pulse-width (which scales as a length). By choosing  $C = 0$ , we solve the regularity constraint trivially and also avoid having to deal with Bessel functions of the second kind. These same choices were discussed by Bonnor[6] and later led to Weber-Wheeler waves in the Einstein-Rosen case.[7] The basic technique for evaluating the integrals in Eqs. 2 and 4 is also the same as in the Bonnor-Weber-Wheeler case: Use the integral representation of the Bessel function,

$$J_0(z) = \frac{1}{2\pi} \int_{-\pi}^{\pi} e^{iz \sin \phi} d\phi,$$

to turn each integral into a multiple integral and then change the order of integration.

The key result of this paper is the fundamental Bonnor pulse solution

$$W_0(\alpha, r, t) = \alpha \int_0^\infty e^{-\alpha k} J_0(kt) J_0(kr) dk,$$

or, using the integral representation,

$$W_0 = \frac{\alpha}{4\pi^2} \int_{-\pi}^{\pi} d\zeta \int_{-\pi}^{\pi} d\xi \int_0^\infty dk e^{k(-\alpha + it \sin \zeta + ir \sin \xi)}$$

Two of these integrations are essentially the same as the ones for Weber-Wheeler waves and leave just one integration still to be performed:

$$W_0 = \frac{1}{2\pi r} \int_{-\pi}^{\pi} \frac{\alpha}{\sqrt{1+w^2}} d\zeta$$

where  $w$  is defined by

$$w = \frac{\alpha}{r} - i \frac{t}{r} \sin \zeta.$$

This last integration can be put into the form of an elliptic integral

$$W_0 = \frac{\alpha}{\pi \sqrt{r^2 + \alpha^2}} \int_{-1}^1 \frac{dy}{\sqrt{(1-y)(1+y)(1-\rho^* y)(1+\rho y)}}$$

where

$$\rho = \frac{t}{r - i\alpha}.$$

This elliptic integral can be put into Legendre normal form by the bilinear transformation

$$y = \frac{x + ih}{ihx + 1}$$

where

$$h = \frac{1}{2t\alpha} \left( (r^2 - t^2 + \alpha^2) - \sqrt{(r^2 - t^2 + \alpha^2)^2 + 4t^2\alpha^2} \right) \quad (7)$$

and yields the solution:

$$W_0 = BK(m) \quad (8)$$

where  $K$  is the complete elliptic integral of the first kind, the elliptic modulus  $m$  is

$$m = h \frac{h\alpha + t}{ht - \alpha} \quad (9)$$

and

$$B(\alpha, r, t) = \frac{2\alpha}{\pi} \sqrt{\frac{h}{t(ht - \alpha)}}. \quad (10)$$

### B. Asymptotic properties and amplification by the expansion of the universe

The elliptic function  $K(m)$  is just the period of a unit circular pendulum with  $m = \sin^2(\theta_{\max}/2)$  where  $\theta_{\max}$  is the maximum angle from the bottom of the pendulum swing. For a large range of values of  $m < 1$  that period is nearly constant and almost equal to  $\pi/2$ . However, the function  $K(m)$  has a logarithmic singularity at  $m = 1$ , which corresponds to the circular pendulum balancing upside-down at the ends of its swing. In the near-field zone of the solution, where  $r$  and  $t$  are comparable to the size parameter  $\alpha$ , one finds that  $m$  is sufficiently smaller than 1 for  $K(m)$  to be essentially constant. In that region, the function  $B$  describes the pulse quite accurately and the resulting behavior is very similar to the Weber-Wheeler pulse solution. However, as  $r$  and  $t$  increase, the function  $m$  rapidly approaches 1 near  $r = t$ . The logarithmic singularity of  $K(m)$  then comes to dominate the solution, which no longer behaves like a Weber-Wheeler pulse.

The peak of a Bonnor pulse occurs at  $r = t$  so the peak value can be found by evaluating  $W_0(1, r, r)$ . Equations (7), (8), (9), and 10 then simplify to

$$rW_0(1, r, r) = \frac{2}{\pi} \sqrt{\frac{\sqrt{1+4r^2}-1}{\sqrt{1+4r^2}+1}} K\left(\frac{1}{2r^2} \frac{\sqrt{1+4r^2}-1}{\sqrt{1+4r^2}+1} (2r^2+1-\sqrt{1+4r^2})\right).$$

An expansion of this expression, using the asymptotic form of the elliptic function then yields

$$rW_0(1, r, r) = \frac{1}{\pi} (2 \ln 4 - \ln 2 + \ln r) + O(r^{-2}, r^{-2} \ln r)$$

where the terms proportional to  $r$  and  $r \ln r$  have cancelled out. The dominant behavior of the peak is then given by

$$W_0(1, r, r) = \frac{2}{\pi} \frac{\ln r}{r} + O(r^{-1})$$

The shapes of these pulses provide an explanation for their anomalous behavior. Figure 2 shows a series of snapshots of a pulse at successive times. This figure plots  $tW_0(r, t)$  so that an  $r = t$  peak with the expected  $1/r$  behavior would appear as a succession of peaks rising to a constant level. The  $\ln r/r$  behavior is quite evident in the way that the peaks grow with  $r$ . However, even more evident is the fact that these pulses are not localized and fill the  $r = t$  event horizon of the universe. The length scale  $\alpha = 1$  of the solution characterizes only the radius of curvature of the sharp peak of the pulse and not the overall width of the pulse, which is always comparable to the horizon size,  $t$ . Thus, these pulses experience a weak amplification because they always have a characteristic period that matches the time

scale of the expansion.

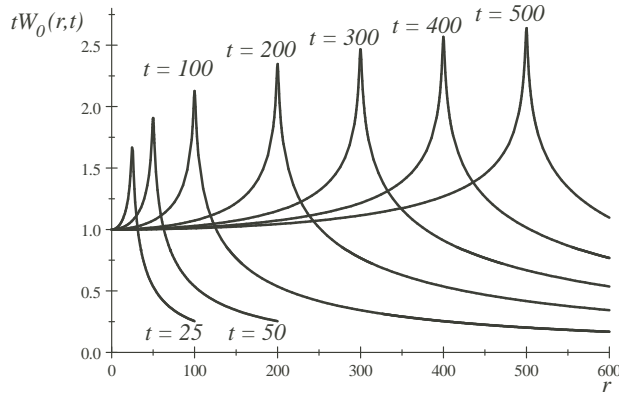


FIG. 2 Snapshots of a pulse at successive times. The pulse grows because it fills the event horizon and is amplified by the expansion.

#### IV. LOCALIZED, REGULAR PULSES

##### A. Differences of scaled solutions

To obtain pulses that are not amplified by the expansion, take advantage of scale invariance and note that, if  $W_0(r, t)$  is a solution, then so are the scaled solutions  $W_0(br, bt)$  for any constant  $b$ . The differences

$$U_b(r, t) = \frac{\pi}{\ln b} (bW_0(br, bt) - W_0(r, t))$$

will then also be solutions. These difference solutions are chosen so that the  $\ln r/r$  terms cancel, leaving only a  $1/r$  behavior for large values of  $r$ . The normalization is chosen so that the peak value will approach exactly  $1/r$ . Figure 3 shows a series of snapshots of the difference solution for  $b = 2$ . The  $r = t$  peak in  $tU_2(r, t)$  now approaches a constant value of 1, indicating a  $1/r$  dependence that is no surprise since we built that property in to these solutions. As a confirmation that we understand how these pulses work, the figure also shows that the peak is clearly localized near  $r = t$  and has a width that is comparable to the length scale  $\alpha$  (taken to be 1 in the figure). For these pulses, the characteristic time is a constant  $\alpha/c$  so that there is no continuing resonance with the expansion to amplify them. By choosing peaks that are not amplified, we have obtained peaks that are also localized.

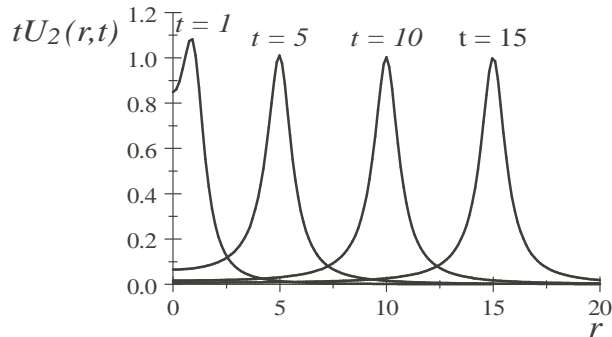


FIG. 3 Snapshots of a difference pulse at successive times. This type of pulse is localized and falls off as  $1/r$ .

Another way to view the behavior of these difference solutions is to plot the peak values or  $rW$  versus  $r$  for different values of the scaling parameter, as in Fig. 4. There it can be seen that all of these solutions begin a  $1/r$  behavior within a distance  $\alpha$  (taken to be 1 in the figure).

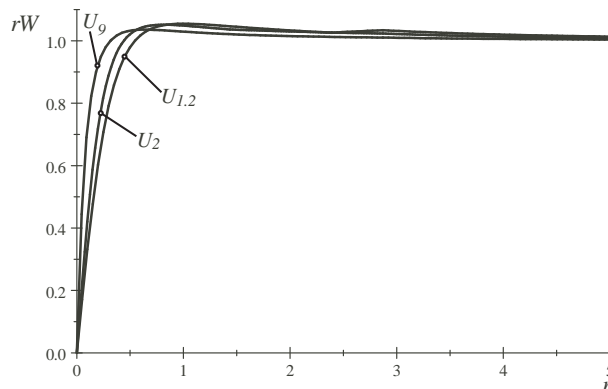


FIG. 4 Peak values of difference solutions for three values of the scaling parameter.

### B. Notched waves

Each of the difference solutions consists of a single pulse. More complex solutions with multiple pulses can be constructed by combining difference solutions with different scaling factors. Figure 5 shows a snapshot of a solution that consists of the difference

$$W = U_2 - U_9$$

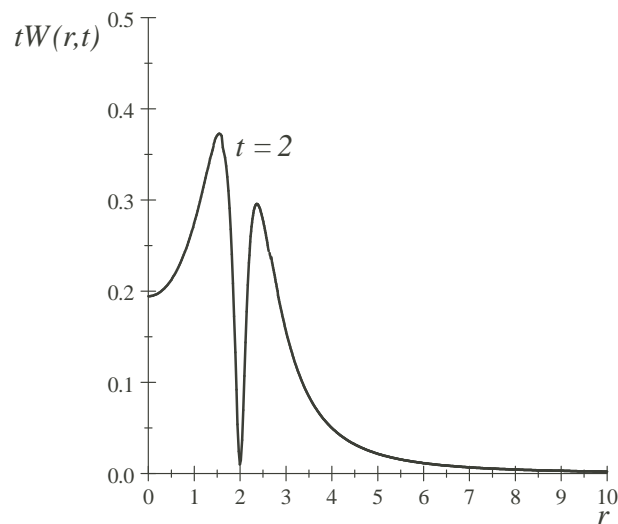


FIG. 5 A “notched wave” formed by the difference of scaled solutions  $U_2 - U_9$ .

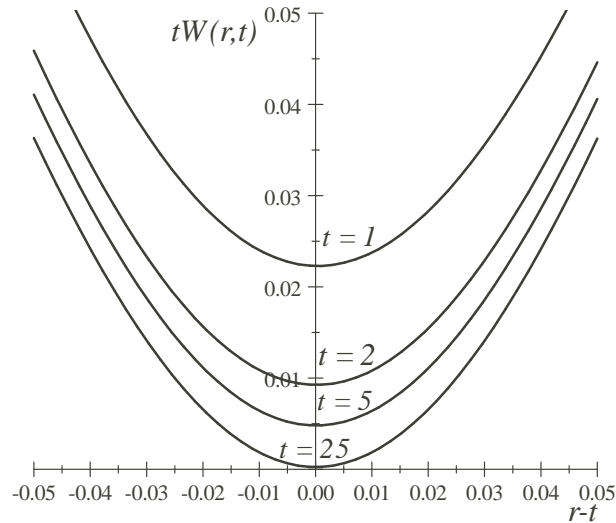


FIG. 6. Magnified view of the bottom of the "notch" in the  $U_2 - U_9$  solution at four values of the time,  $t$ .

The most striking feature of this solution is a deep and narrow trough or "notch" between two maxima of the gravitational wave amplitude  $W$ . As the magnified view in Fig. 6 shows, the bottom of this notch is actually smooth but the second derivative of  $W$ , and thus the spacetime curvature, is extremely large there. As Fig. 6 also shows, the bottom of the notch moves downward to the axis at large values of  $t$ . This type of exact solution could be used as a sensitive test of a numerical simulation's ability to reproduce exact waveforms in the far-field region by observing the behavior of the notch there.

## V. DISCUSSION

The localized, regular solutions described here represent short pulses of gravitational radiation that spread in a way that mimics radiation from a compact source in three dimensions. The waves are cylindrical, which accounts for spreading in two dimensions. The waves inhabit a universe that is expanding along the cylindrical axis, which accounts for spreading in the remaining dimension. To use one of these solutions to test the far-field behavior of a numerical simulation of spacetime dynamics, one would evaluate the solution at a time  $t < \alpha$  to find initial values of the metric functions and their time derivatives as functions of  $r$  and would then use the numerical simulation scheme to evolve the spacetime to  $t \gg \alpha$ . In the simplest case, where no explicit gravitational wave extraction scheme is used, the wave pulse would just run off the edge of the numerical evaluation grid, where one would typically have some sort of damping scheme to minimize spurious reflection. A comparison to the exact solution would then make it possible to see just how much spurious reflection actually occurs. More complex schemes such as Cauchy Characteristic Matching[2, 3, 4, 5] could be tested in a similar way for unwanted reflections from their matching regions. The notched solutions should be particularly useful for finding accumulated numerical errors in the far-field waveform produced by any of these simulation schemes.

- 
- [1] R. H. Gowdy and B. D. Edmonds, Phys. Rev. D **75**, 084011 (2007).
  - [2] C. J. S. Clarke, R. A. d'Inverno, and J. A. Vickers, Phys. Rev. D **52**, 6863 (1995).
  - [3] M. R. Dubal, R. A. D'Inverno, and C. J. S. Clarke, Phys. Rev. D **52**, 6868 (1995).
  - [4] M. Babiuc, B. Szilágyi, I. Hawke, and Y. Zlochower, Class. Quantum Grav. **22**, 5089 (2005), arXiv:gr-qc/0501008 v2.
  - [5] G. Calabrese, Class. Quantum Grav. **23**, 5439 (2006).
  - [6] W. B. Bonnor, J. Math. and Mech. **6**, 203 (1957).
  - [7] J. Weber and J. A. Wheeler, Rev. Mod. Phys. **29**, 509 (1957), includes a letter from M. Fierz pointing out the conical nature of the asymptotic geometry of a cylindrical wave spacetime.

- [8] C. W. Misner, in *Relativity Theory and Astrophysics I: Relativity and Cosmology*, edited by J. Ehlers (American Mathematical Society, Providence, 1967), pp. 160–169.
- [9] C. W. Misner, *J. Math. Phys.* **4**, 924 (1963).
- [10] A. H. Taub, *Ann. Math.* **53**, 472 (1951).
- [11] J. Bičák and B. Schmidt, *Phys. Rev. D* **40**, 1827 (1989).